Protonium formation in collinear collisions between antiprotons and hydrogen molecular ions: Quantum-classical hybrid method versus adiabatic approximation

Kazuhiro Sakimoto*
Institute of Space and Astronautical Science, Japan Aerospace Exploration Agency, Yoshinodai, Sagamihara 229-8510, Japan
(Received 8 April 2003; published 9 April 2004)

A quantum-classical hybrid (or semiclassical) method is applied to protonium formation $\bar{p}+H_2^+ \rightarrow \bar{p}\bar{p}+H$ and dissociation $\bar{p}+H_2^+ \rightarrow \bar{p}+p+H$ at kinetic energies up to 200 eV. The electronic motion is accurately solved quantum mechanically, while the motion of the heavy particles $\bar{p}$ and p is described by classical mechanics. The $\bar{p}$-p-p collinear configuration is assumed as a preliminary to three-dimensional calculations, and to assess the validity of the adiabatic approximation. Vibrational excitation to the dissociative continuum is crucial in $\bar{p}\bar{p}$ formation in contrast to the importance of electron emission for the *atomic*-hydrogen target. For this reason, $\bar{p}\bar{p}$ formation occurs efficiently even well beyond the ionization threshold if the target is a molecule.

DOI: 10.1103/PhysRevA.69.042710 PACS number(s): 34.90.+q, 36.10.−k, 34.50.Fa

I. INTRODUCTION

Antiprotonic atoms afford an opportunity to study extraordinary atomic physics and the fundamental principles of physics by the way of matter-antimatter symmetry [1,2]. This has stimulated much recent efforts toward high-resolution spectroscopy of antiprotonic atoms, such as antihydrogen ($\bar{H}=e^+\bar{p}$), protonium ($\bar{p}\bar{p}$), and antiprotonic helium ($He^{2+}e\bar{p}$) [3–6]. For such spectroscopy, we need to know which type of atomic or molecular collision processes can serve as a means to produce enough number of antiprotonic atoms.

In the present paper, we develop a theoretical study of the formation process of protonium atoms in antiproton and molecule collisions. So far, a lot of theoretical studies have been made for protonium formation [7–17]. However, most of them are for collisions with hydrogen atoms, i.e., $\bar{p}+H \rightarrow \bar{p}\bar{p}+e$. The only theoretical attempt for a molecular target appears to be that of the system $\bar{p}+H_2$ by Cohen [10,11], using fermion molecular dynamics (FMD). The FMD method is similar to a classical trajectory Monte Carlo (CTMC) method, but takes some quantum correction into account.

If the target is a neutral hydrogen atom, electronically bound states are absent for a close approach of an antiproton, and the electron emission plays a key role in the protonium formation. For positive-ion targets, however, the electrons are tightly bound even when the antiproton comes close to the nucleus. For this reason, the electronic excitation channels are considered to be negligible when the kinetic energy is low [20]. In addition, the successful application of the adiabatic (Born-Oppenheimer) approximation to the study of the moleculelike structure in antiprotonic helium ($=\bar{p}+He^+$) [21,22] suggests that it may work nicely also for the system of an antiproton and a molecular (positive) ion. Then, the problem is similar to chemical reactions on a single potential-energy surface (PES).

In the present paper, we choose an ionic target and consider the processes

$$\bar{p}+H_2^+ \rightarrow \bar{p}\bar{p}+H \quad (1)$$

$$\rightarrow \bar{p}+p+H \quad (2)$$

at kinetic energies $\ll 1$ keV. If the adiabatic approximation is satisfactory, these processes can be treated as three-body ($\bar{p},p,H$) collisions on the adiabatic PES. The purpose of the present paper is to assess the validity of the adiabatic approximation for the present system. To take account of the nonadiabatic process, we introduce a quantum-classical (QC) hybrid (i.e., semiclassical) method, in which the heavy particle motions are described by classical mechanics while the electronic motions are accurately described by quantum mechanics. The QC method was applied to the calculations of protonium formation and muon capture ($\mu^-+H \rightarrow \mu^- p+e$) for the hydrogen-atom target [14,18]. The results have been compared in detail with those of full quantal calculations [15,16,19], which have clarified under which circumstances the QC method is reasonably accurate. Although the QC approximation makes the collision calculation much manageable, a full description of all the degrees of freedom is still laborious. Here, we further assume a collinear configuration for the three heavy particles ($\bar{p},p,p$), as is often the case with chemical reaction studies. No such restrictions are imposed on the electronic motion. The collinear treatment is very useful for the present purpose, and is also an important preliminary to a subsequent three-dimensional (3D) study of the processes (1) and (2) using the adiabatic PES [23].

II. THEORY

A. Adiabatic electronic states of H_2^+

As defined in Fig. 1, let $\mathbf{s}_1$ and $\mathbf{s}_2$ be the position vectors of the electron measured from the outer and inner protons, and $\mathbf{s}$ from the midpoint between the two protons. No use is made of the adiabatic approximation for the electronic states of the hydrogen molecular ion H_2^+ in the present QC calculation. Nevertheless, it is convenient to start from the account

*Email address: sakimoto@pub.isas.jaxa.jp

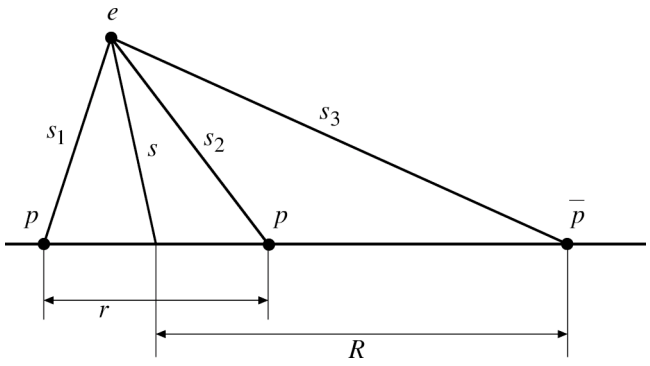

FIG. 1. Coordinates of the $\bar{p}+H_2^+$ system.

of this approximation, which very accurately describes electronic states of H_2^+. The Schrödinger equation for the electron for a fixed internuclear distance r is given by

$$\tilde{H}_0\Phi = \epsilon(r)\Phi, \tag{3}$$

where

$$\tilde{H}_0 = -\frac{1}{2}\nabla_s^2 - \frac{1}{s_1} - \frac{1}{s_2} \tag{4}$$

and $\epsilon(r)$ is the electronic energy. Here and in the following, we use atomic units unless otherwise stated. To take account of the two-center Coulomb nature of the molecule, we introduce coordinates (ξ, η) defined by

$$\xi = -r + s_1 + s_2, \quad 0 \leqslant \xi < \infty, \tag{5}$$

$$\eta = \frac{-s_1 + s_2}{r}, \quad -1 \leqslant \eta \leqslant +1, \tag{6}$$

which are similar to spheroidal [24–26] or perimetric coordinates [27]. Using the coordinates (ξ, η) and assuming a vanishing angular momentum around the internuclear axis r, we can express the Hamiltonian $\tilde{H}_0$ as

$$\tilde{H}_0 = \frac{2}{G}\left[-\frac{\partial}{\partial\xi}\xi(2r+\xi)\frac{\partial}{\partial\xi} - \frac{\partial}{\partial\eta}(1-\eta^2)\frac{\partial}{\partial\eta} - 2(r+\xi)\right], \tag{7}$$

where

$$G(r,\xi,\eta) = \xi(2r+\xi) + r^2(1-\eta^2). \tag{8}$$

The volume element is given by $dv = 1/8 G d\xi d\eta$.

Although Eq. (3) with the Hamiltonian (7) is separable with respect to ξ and η [24], here we consider another approach that is more convenient for later use in the following section. A definition of $\phi(\xi, \eta)$ by

$$\Phi(\xi,\eta) = [\xi(2r+\xi)]^{-1/2}\phi(\xi,\eta) \tag{9}$$

casts Eq. (3) into a form

$$(\tilde{T} + U)\phi = \epsilon\frac{G}{2\xi(2r+\xi)}\phi, \tag{10}$$

where

$$\tilde{T} = -\frac{\partial^2}{\partial\xi^2} - \frac{1}{4\xi^2} - \frac{1}{\xi(2r+\xi)}\frac{\partial}{\partial\eta}(1-\eta^2)\frac{\partial}{\partial\eta}, \tag{11}$$

$$U(r,\xi,\eta) = \frac{4r+\xi}{4\xi(2r+\xi)^2} - \frac{2(r+\xi)}{\xi(2r+\xi)}. \tag{12}$$

We use a discrete-variable-representation (DVR) technique [28–30], and calculate the wave function directly on the grid points defined in the configuration space. The η part of the operator $\tilde{T}$ is identical to the differential operator for the Legendre polynomials $P_n(x)$. Therefore, the zero points $\eta_j (j=1,2,\ldots,M)$ of $P_{n=M}(\eta)$ are chosen to be the η grid points. The ξ part of the operator $\tilde{T}$ has a singularity $-1/4\xi^2$ as $\xi \to 0$, which could, in principle, raise a severe difficulty in the numerical calculation. Fortunately, however, the generalized Laguerre polynomials $L_n^{(\alpha)}(x)$ with $\alpha=1$ may be used, in practice, to avoid this singularity [28]. Therefore, we construct the ξ grid from the zero points ξ_i $(i=1,2,\ldots,N)$ of $L_{n=N}^{(\alpha=1)}(\xi)$.

We expand the eigenfunction ϕ as

$$\phi(\xi,\eta) = \sum_{ij}\phi_{ij} f_i(\xi) g_j(\eta) \tag{13}$$

in terms of the DVR basis functions

$$f_i(\xi) = \frac{[W(\xi)]^{1/2} L_N^{(1)}(\xi)}{\omega_i^{1/2}[dL_N^{(1)}(\xi_i)/d\xi](\xi-\xi_i)}, \tag{14}$$

$$g_j(\eta) = \frac{P_M(\eta)}{\omega_j^{1/2}[dP_M(\eta_j)/d\eta](\eta-\eta_j)}. \tag{15}$$

Here, $W(\xi) = \xi e^{-\xi}$ is the weight function of $L_N^{(1)}(\xi)$, ω_i the quadrature weight of $L_N^{(1)}(\xi)$, and ω_j that of $P_M(\eta)$. The coefficients ϕ_{ij} are defined by

$$\phi_{ij} = \left[\frac{\omega_i\omega_j}{W(\xi_i)}\right]^{1/2}\phi(\xi_i\eta_j). \tag{16}$$

Using the orthogonal properties of $f_i(\xi)$ and $g_j(\eta)$ [31] and the Gaussian quadrature rule, we can derive from Eq. (10) linear algebraic equations for ϕ_{ij}:

$$\sum_{i'j'} T_{ij,i'j'}\phi_{i'j'} + U(r,\xi_i,\eta_j)\phi_{ij} = \epsilon\frac{G(r,\xi_i,\eta_j)}{2\xi_i(2r+\xi_i)}\phi_{ij}, \tag{17}$$

where explicit forms of the matrix elements

$$T_{ij,i'j'} = \int f_i(\xi) g_j(\eta_j)\tilde{T} f_{i'}(\xi) g_{j'}(\eta) d\xi d\eta \tag{18}$$

have been obtained by Baye and Heenen [28] and Sakimoto [30].

The introduction of the two-center coordinates (ξ,η) is essential in the efficient calculation of the electronic state. If we used single-center coordinates such as polar coordinates, the DVR calculation of the electronic state would be grossly inefficient because at least one of the Coulomb singularities is impossible to handle properly. Unlike the usual dimensionless spheroidal coordinates, the variable ξ defined by Eq. (5) has the dimension of the length. This has an advantage because the electronic wave function is always well localized around the protons, as seen later. Large ξ is unimportant, and we may use the same value of N over the whole range of the internuclear distance r. If we defined ξ by $(-r+s_1+s_2)/r$, then larger values of N would have to be chosen for larger r. Furthermore, we may set a cutoff value ξ_c for ξ to carry out calculations with a smaller number of grid points, i.e., $i=1,2,\ldots,N_c<N$, where $\xi_{N_c}\simeq\xi_c$.

B. Electronic motion in the QC method for $\bar{p}+H_2^+$

Now we turn to the collision system involving four particles $(\bar{p},p,p,e)$. The quantal equation of the electronic motion is solved in a numerically accurate manner *without the adiabatic approximation*. The three heavy particles are assumed to preserve a collinear configuration as shown in Fig. 1, and their positions are described by the Jacobi coordinates (R,r). In the QC method, these coordinates are treated in classical mechanics. Assuming that the time dependence of R and r is known, we solve the time-dependent Schrödinger equation for the electron

$$i\frac{\partial}{\partial t}\Psi(\xi,\eta,t)=\tilde{H}_e\Psi(\xi,\eta,t), \tag{19}$$

where $\tilde{H}_e$ is the electronic part of the Hamiltonian

$$\tilde{H}_e=\tilde{H}_0+V_{e\bar{p}} \tag{20}$$

with the Coulomb potential

$$V_{e\bar{p}}(R,r,\xi,\eta)=\frac{1}{s_3}=\left\{\left(R-\frac{r}{2}\right)^2+\frac{1}{4}(r+\xi+r\eta)^2+\left(R-\frac{r}{2}\right)[r+(r+\xi)\eta]\right\}^{-1/2} \tag{21}$$

between the electron and the antiproton. Since this interaction is repulsive, the two centers at the protons are more important than the third center at the antiproton in the calculation of the electronic state. Therefore, the coordinates (ξ,η) are useful also for the present four-body system. Putting

$$\Psi(\xi,\eta,t)=[\xi(2r+\xi)]^{-1/2}\psi(\xi,\eta,t) \tag{22}$$

in a manner similar to Eq. (9), we have

$$\frac{iG}{2\xi(2r+\xi)}\frac{\partial\psi}{\partial t}=\left\{\tilde{T}+U+\frac{G}{2\xi(2r+\xi)}\left[V_{e\bar{p}}+\frac{idr/dt}{2r+\xi}\right]\right\}\psi. \tag{23}$$

Since the adiabatic approximation is accurate for the electronic state of the molecule before the collision, the initial condition $\psi(t=0)$ may be given by

$$\psi(\xi,\eta,t=0)=\phi(\xi,\eta). \tag{24}$$

The time evolution of $\psi(t)$ is studied by using a DVR technique similar to that explained in Sec. II A. The wave function ψ is expanded as

$$\psi(\xi,\eta,t)=\sum_{ij}\psi_{ij}(t)f_i(\xi)g_j(\eta), \tag{25}$$

where

$$\psi_{ij}(t)=\left[\frac{\omega_i\omega_j}{W(\xi_i)}\right]^{1/2}\psi(\xi_i\eta_j,t). \tag{26}$$

Equation (25) substituted into Eq. (23) leads to time-dependent linear equations for $\psi_{ij}(t)$:

$$i\frac{\partial\psi_{ij}}{\partial t}=\frac{2\xi_i(2r+\xi_i)}{G(r,\xi_i,\eta_j)}\left[\sum_{i'j'}T_{ij,i'j'}\psi_{i'j'}+U(r,\xi_i,\eta_j)\psi_{ij}\right]+\left[V_{e\bar{p}}(R,r,\xi_i,\eta_j)+\frac{idr/dt}{2r+\xi_i}\right]\psi_{ij}. \tag{27}$$

If the electron escape (or ionization) is negligible, it suffices to use only the grid points $i=1,2,\ldots,N_c<N$ of ξ in Eq. (27).

C. Classical trajectories of the heavy particles

The Hamiltonian of the whole system $\bar{p}+H_2^+$ is

$$\tilde{H}=\frac{1}{2\mu}P_R^2+\frac{1}{2m}P_r^2+\tilde{H}_e+V_{pp\bar{p}}, \tag{28}$$

where μ (m) is the reduced mass of $\bar{p}+H_2^+$ $(p+H)$, and P_R (P_r) the momentum conjugate to R (r). The potential $V_{pp\bar{p}}=V_{pp\bar{p}}(R,r)$ is the sum

$$V_{pp\bar{p}}=\frac{1}{r}-\frac{1}{R+r/2}-\frac{1}{R-r/2}+\frac{(L+1/2)^2}{2m(R-r/2)^2} \tag{29}$$

of the Coulomb potentials for the three-body system $(p,p,\bar{p})$ and the centrifugal potential between the inner proton and the antiproton. The introduction of the artificial centrifugal term with the Langer modification is to avoid the Coulomb singularity in $-(R-r/2)^{-1}$ occurring at $R=r/2$ in the collinear collision. The quantity L may also be regarded as the angular-momentum quantum number of the produced protonium.

In the QC method, there is no unique way to determine the time dependence of the classical variables $R(t)$ and $r(t)$. Here, we adopt common trajectories as in previous studies [14,18] by using the equations of motion

$$\frac{dR}{dt}=\frac{P_R}{\mu}, \tag{30a}$$

$$\frac{dP_R}{dt} = -\left\langle \Psi \left| \frac{\partial \tilde{H}}{\partial R} \right| \Psi \right\rangle \langle \Psi | \Psi \rangle^{-1}$$

$$= -\left\langle \Psi \left| \frac{\partial V_{ep^-}}{\partial R} \right| \Psi \right\rangle \langle \Psi | \Psi \rangle^{-1} - \frac{\partial V_{pp\bar{p}^-}}{\partial R}, \quad (30b)$$

$$\frac{dr}{dt} = \pm \left\{ \frac{2}{m} \left[E_{\rm tot} - \frac{1}{2\mu} P_R^2 - \frac{\langle \Psi | \tilde{H}_e | \Psi \rangle}{\langle \Psi | \Psi \rangle} - V_{pp\bar{p}^-}, \right] \right\}^{1/2}, \quad (30c)$$

with the total energy $E_{\rm tot}=E+E_0$, E being the initial center-of-mass kinetic energy $[=(1/2\mu)P_R^2(t=0)]$ and E_0 being the energy of the quantum-mechanical ground vibrational state.

D. Adiabatic potential-energy surface of $\bar{p}+H_2^+$

For examining the validity of the adiabatic approximation by comparison with the nonadiabatic QC calculation, here we discuss the ground adiabatic electronic state of the system $\bar{p}+H_2^+$, obtained by diagonalizing the Hamiltonian (20) for each fixed R and r, i.e.,

$$\tilde{H}_e \Theta(\xi, \eta) = \epsilon_{\rm ad}(R,r)\Theta(\xi, \eta). \quad (31)$$

The numerical method of diagonalization is the same as explained in Sec. II A. The adiabatic electronic energy $\epsilon_{\rm ad}(R,r)$ satisfies relations

$$\lim_{R \to r/2} \epsilon_{\rm ad}(R,r) = -\tfrac{1}{2} \quad (32)$$

and

$$\lim_{R \to \infty} \epsilon_{\rm ad}(R,r) = \epsilon(r). \quad (33)$$

The PES is given by

$$V_{\rm ad}(R,r) = \epsilon_{\rm ad}(R,r) + V_{pp\bar{p}}(R,r), \quad (34)$$

on which the processes (1) and (2) will be considered in the adiabatic approximation. Then, we obtain the classical trajectories $R(t)$ and $r(t)$ by solving equations

$$\frac{dR}{dt} = \frac{P_R}{\mu}, \quad (35a)$$

$$\frac{dP_R}{dt} = -\frac{\partial V_{\rm ad}}{\partial R}, \quad (35b)$$

$$\frac{dr}{dt} = \frac{P_r}{m}, \quad (35c)$$

$$\frac{dP_r}{dt} = -\frac{\partial V_{\rm ad}}{\partial r}. \quad (35d)$$

III. NUMERICAL CALCULATIONS

Table I shows the convergence of the electronic energies $\epsilon(r)$ of H_2^+ with respect to N, M, and ξ_c. The last line contains accurate numerical results obtained by series expansion of the separable solution [25,26]. A choice of $N=200$, $M=6$, and $\xi_c=10$ is seen to yield energies with absolute errors $|\Delta\epsilon(r)|$ less than 0.006 except for the smallest r of 0.1 [for which $|\Delta\epsilon(0.1)|=0.01$] and the largest r of 20.0 [$|\Delta\epsilon(20.0)|=0.05$]. The values $N=200$, $M=8$, and $\xi_c=15$ were used in the collision calculations, since the increase of M into 8 reduces $|\epsilon(20.0)|$ by a factor of ~ 6, and since accurate electronic energies up to $r \simeq 10.0$ is sufficient for the purpose of establishing the criterion for dissociation to have occurred.

The convergence rate of the adiabatic energies $\epsilon_{\rm ad}(R,r)$ of the system $\bar{p}+H_2^+$ with respect to N, M, and ξ_c was found to be similar to that of $\epsilon(r)$ of H_2^+. A choice $N=200$, $M=12$, and $\xi_c=15$ was made to calculate $\epsilon_{\rm ad}(R,r)$, shown in Fig. 2, at 270×270 points in a region ($R \leqslant R_0=20, r \leqslant r_0=40$), and interpolation between these points was made by using quadratic polynomials for the classical-trajectory calculation of Eq. (35); $\epsilon_{\rm ad}(R \geqslant R_0, r)$ was assumed to be Coulombic.

The adiabatic PES $V_{\rm ad}(R,r)$ *excluding* the centrifugal potential is presented in Fig. 3. Here, the reactant channel $\bar{p}+H_2^+$ may be understood as the motion along the valley running along the R axis at $r \sim 2$. The bottomless valley along $R=r/2$, representing the product channel $\bar{p}p+H$, originates in the Coulomb singularity. The plateau extending toward large values of r and $R-r/2$ leads to the dissociation channel $\bar{p}+p+H$.

Figure 4 shows $V_{\rm ad}(R,r)$ for $L=60$. The Coulomb singularity is absent here owing to the repulsive centrifugal potential. The Coulomb plus centrifugal potential for the protonium has a minimum, which becomes nearly equal to the potential minimum of the hydrogen molecular ion when $L=L_c \sim 67$. For $L<L_c$, therefore, the system is more stable to form a protonium atom than to form a hydrogen molecular ion, that is, protonium formation is expected to be important at low kinetic energies.

We chose $N=200$, $M=8$, and $\xi_c=15$ in the QC calculation. This cutoff value ξ_c gives $N_c=34$ for $N=200$. From the dependence of the probability $P_{\bar{p}p}$ of protonium formation on the choice of the numerical parameters (see Table I), the absolute error in $P_{\bar{p}p}$ is estimated to be less than 0.01. The value $\xi_c=15$ is large enough for $E \ll 1$ keV since the electron escape is negligible. For $E \gtrsim 1$ keV, however, a larger cutoff value must be chosen.

Using an angle variable q of the initial molecular vibration defined in terms of the action variable J by

$$q = \frac{\partial}{\partial J} \int^r P_r dr, \quad (36)$$

the probability of protonium formation is expressible as

$$P_{\bar{p}p} = \frac{1}{2\pi} \int_{\bar{p}p} dq, \quad (37)$$

where the integral is to be calculated for the initial conditions that lead to protonium formation in the trajectory calculations. If the energy of the $\bar{p}$-p system,

TABLE I. Variation of the electronic energies $\epsilon(r)$ (in a.u.) of H_2^+ with respect to N, M, and ξ_c (in a.u.) for several values of r (in a.u.). Acc.: Accurate values obtained by series expansion of the separable solution.

r	0.1	0.5	1.0	5.0	10.0	20.0
N			$M=6,\ \xi_c=15$			
50	−2.0221	−1.7174	−1.4296	−0.7148	−0.5885	−0.4979
100	−1.9991	−1.7260	−1.4403	−0.7195	−0.5928	−0.5012
200	−1.9884	−1.7304	−1.4460	−0.7219	−0.5950	−0.5029
300	−1.9849	−1.7319	−1.4479	−0.7227	−0.5958	−0.5035
400	−1.9832	−1.7727	−1.4488	−0.7231	−0.5962	−0.5038
500	−1.9822	−1.7331	−1.4494	−0.7234	−0.5964	−0.5039
600	−1.9815	−1.7335	−1.4500	−0.7235	−0.5966	−0.5040
M			$N=200,\ \xi_c=15$			
2	−0.1988	−1.7294	−1.4402	−0.6266	−0.3796	−0.2172
4	−1.9884	−1.7304	−1.4460	−0.7169	−0.5464	−0.3860
6	−1.9884	−1.7304	−1.4460	−0.7219	−0.5950	−0.5029
8	−1.9884	−1.7304	−1.4460	−0.7219	−0.5981	−0.5418
10	−1.9884	−1.7304	−1.4460	−0.7219	−0.5982	−0.5473
12	−1.9884	−1.7304	−1.4460	−0.7219	−0.5982	−0.5476
ξ_c			$M=6,\ N=200$			
5	−1.9825	−1.7238	−1.4370	−0.7015	−0.5724	−0.4822
10	−1.9884	−1.7304	−1.4460	−0.7218	−0.5949	−0.5027
15	−1.9884	−1.7304	−1.4460	−0.7219	−0.5950	−0.5029
20	−1.9884	−1.7304	−1.4460	−0.7219	−0.5950	−0.5029
Acc.	−1.9782	−1.7350	−1.4518	−0.7244	−0.6006	−0.5500

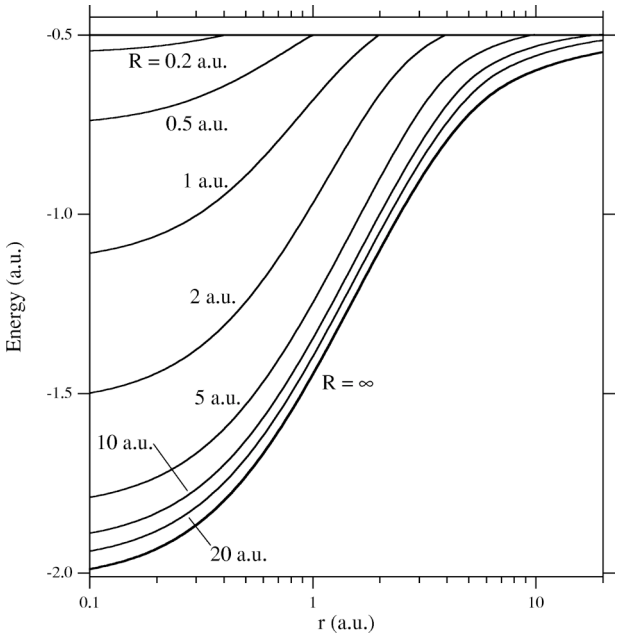

FIG. 2. Adiabatic energies $\epsilon_{ad}(R,r)$ of $\bar{p}+H_2^+$.

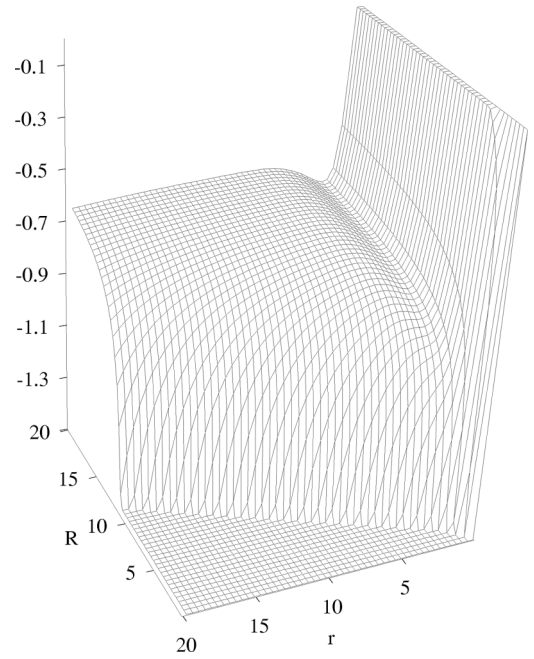

FIG. 3. Adiabatic potential-energy surface $V_{ad}(R,r)$ (in a.u.) of $\bar{p}+H_2^+$, without inclusion of the centrifugal potential, as a function of the distances R and r (in a.u.).

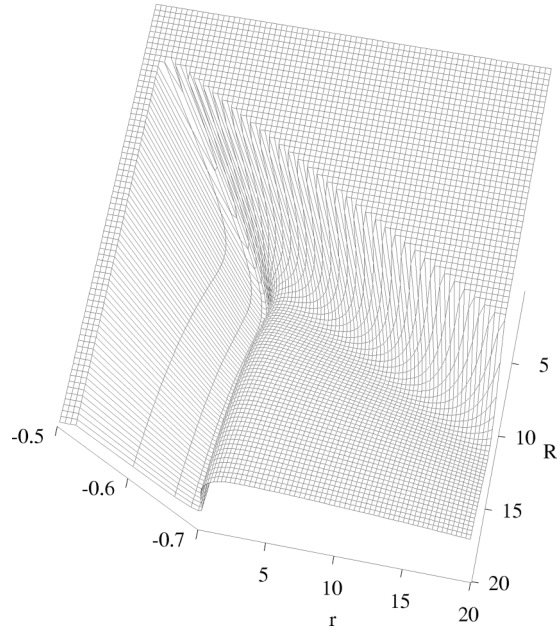

FIG. 4. Adiabatic potential-energy surface $V_{ad}(R,r)$ (in a.u.) of $\bar{p}+H_2^+$ for $L=60$ as a function of the distances R and r (in a.u.).

$$E_{\bar{p}p} = \frac{m}{2}\left(\frac{dR}{dt} - \frac{1}{2}\frac{dr}{dt}\right)^2 - \frac{1}{R-r/2} + \frac{(L+1/2)^2}{2m(R-r/2)^2} \quad (38)$$

becomes a negative constant after the collision, the protonium is known to have been formed in the collision.

IV. RESULTS AND DISCUSSION

The time evolution of the distances R and $r/2$ and of the energy $E_{\bar{p}p}$ of the $\bar{p}$-p pair is illustrated in Fig. 5 for $E=10$ eV and $L=60$ and for two typical choices of the initial value $q/2\pi=0.2475$ and 0.7525. The oscillation of $r(t)$ seen at $t<1000$ is due to the molecular vibration before the collision. The minimum of $R(t)$ represents the primary close encounter, occurring between the antiproton and the inner proton (cf. Fig. 1), while the minimum of $r(t)$ occurring soon after that represents the secondary close encounter between the recoil proton and the outer proton. The latter is then knocked off, and consequently the two protons depart from each other, i.e., the molecule breaks up. The momentum transfer from the antiproton to the molecule through these two close encounters is very efficient due to the same mass of the three heavy particles. For $q/2\pi=0.7525$, all the three particles finally get separated from each other, and hence result in dissociation (2). For $q/2\pi=0.2475$, however, the inner proton stays near the antiproton, and protonium formation (1) takes place. These different kinds of events are clearly identified by observing the energy $E_{\bar{p}p}$, which becomes positive for $q/2\pi=0.7525$ and negative for $q/2\pi=0.2475$ after the collision.

The time evolution of the electron distributions $\rho_1(\xi,t)$ and $\rho_2(\eta,t)$, defined by

$$\rho_1(\xi,t) = \int |\Psi(\xi,\eta,t)|^2 \frac{G}{8} d\eta \langle\Psi|\Psi\rangle^{-1}, \quad (39a)$$

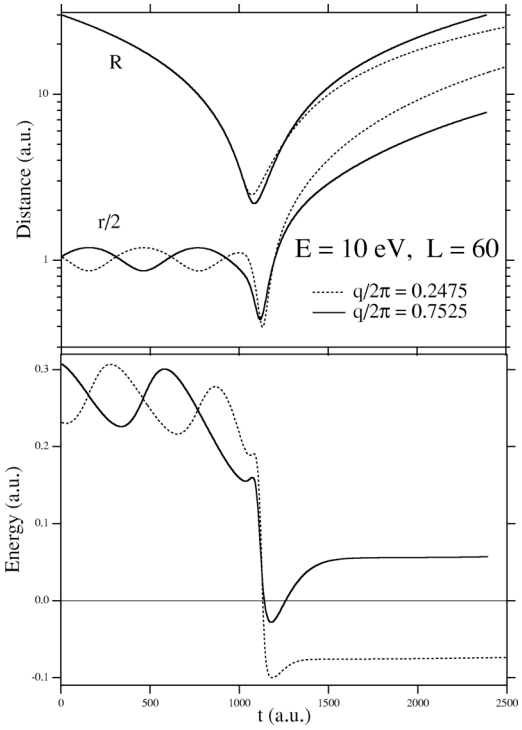

FIG. 5. Time evolution of the distances $R(t)$ and $r(t)/2$ (upper panel) and of the energy $E_{\bar{p}p}(t)$ of the $\bar{p}$-p pair (lower panel) in the quantum-classical calculations for $E=10$ eV, $L=60$, and $R(t=0)=30$ a.u., and for two different initial conditions $q/2\pi=0.2475$ [$r(t=0)=2.1$ a.u., $P_r(t=0)<0$] and $q/2\pi=0.7525$ [$r(t=0)=2.1$ a.u., $P_r(t=0)>0$].

$$\rho_2(\eta,t) = \int |\Psi(\xi,\eta,t)|^2 \frac{G}{8} d\xi \langle\Psi|\Psi\rangle^{-1}, \quad (39b)$$

may be directly monitored in the QC calculation. They are illustrated in Fig. 6 for a protonium formation event ($q/2\pi=0.2475$). A periodic structure is seen in $\rho_1(\xi,t)$ at $t<1000$ because the electron follows the nuclear vibration. After the successive two close encounters ($t\gtrsim1250$), the periodic structure in $\rho_1(\xi,t)$ disappears and the wave packet remains localized around small ξ, while a wave packet in η becomes

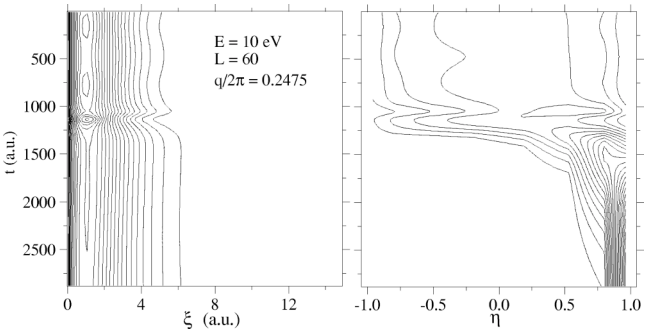

FIG. 6. Time evolution of the electron distributions, $\rho_1(\xi,t)$ (left panel) and $\rho_2(\eta,t)$ (right panel), in the quantum-classical calculation for $E=10$ eV, $L=60$, $R(t=0)=30$ a.u., and $q/2\pi=0.2475$ [$r(t=0)=2.1$ a.u., $P_r(t=0)<0$].

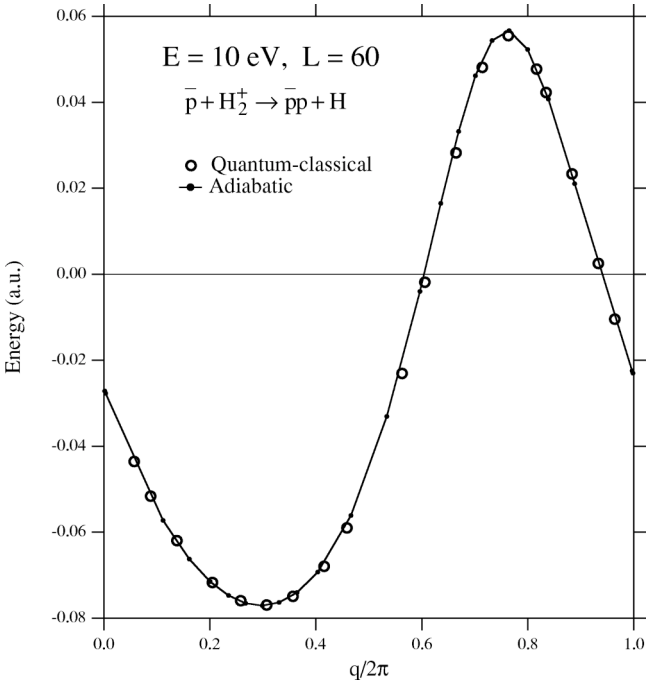

FIG. 7. Final energies $E_{\bar{p}p}$ of the $\bar{p}$-p pair as a function of the initial angle variable q for $E=10$ eV and $L=60$. The results of the quantum-classical and adiabatic-approximation calculations are compared.

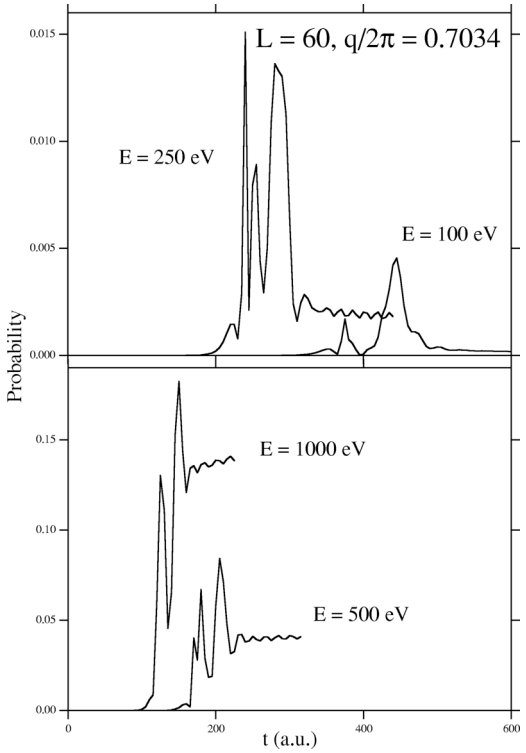

FIG. 8. Time evolution of the nonadiabatic occupation probability $P_{\text{nonad}}(t)$ due to the quantum-classical calculations for $L=60$, $R(t=0)=30$ a.u., and $q/2\pi=0.7034$ $[r(t=0)=2.0$ a.u., $P_r(t=0)<0]$, shown for kinetic energies $E=100$, 250, 500, and 1000 eV.

localized around $\eta=1$. Thus, the electron is bound only by the outer proton after the collision, forming an atomic hydrogen. A very similar time evolution has been found for dissociation ($q/2\pi=0.7525$), although not shown here. The final value of the energy $E_{\bar{p}p}$ calculated by the QC method is plotted versus $q/2\pi$ for $E=10$ eV and $L=10$ in Fig. 7. The positive $E_{\bar{p}p}$ implies no protonium formation, which is seen to occur for $0.60<q/2\pi<0.93$. The inspection of the trajectories reveals that all the events leading to $E_{\bar{p}p}>0$ are dissociative, and nonreactive collisions $\bar{p}+H_2^+ \rightarrow \bar{p}+H_2^+$ never occur.

Figure 7 also includes $E_{\bar{p}p}$ calculated using the adiabatic approximation. The results agree with the QC values very well, supporting the validity of the adiabatic approximation at low energies. To assess the reliability of the adiabatic approximation more directly at other collision energies, we calculate the occupation probability of the nonadiabatic states defined by

$$P_{\text{nonad}}(t) = 1 - |\langle\Theta|\Psi(t)\rangle|^2\langle\Psi|\Psi\rangle^{-1}, \tag{40}$$

where Θ is the adiabatic wave function in Eq. (31). This probability, shown in Fig. 8 for energies $E=100$, 250, 500, and 1000 eV is very small (<0.015) throughout the collision if $E\leqslant 250$ eV, but can exceed 0.1 if $E>500$ eV. This leads to the conclusion that the adiabatic approximation is satisfactory for $E\ll 1000$ eV.

Any significant electronic excitation would deteriorate the common-trajectory method (30) in the QC calculation. Common trajectories were used also for protonium formation in collisions $\bar{p}$+H [15], which is one of the most inappropriate cases for this method because of the significant ionization. Figure 8 assures that electronic excitation is much less important in and common trajectories are much more reliable for $\bar{p}+H_2^+$ than $\bar{p}$+H even at fairly high energies.

The probability (37) of protonium formation for $L=60$ at kinetic energies up to $E=250$ eV is plotted in Fig. 9. That calculated in the adiabatic approximation agrees fairly well with the QC results. The probabilities of dissociation and nonreactive collisions are also included in Fig. 9; only the simpler adiabatic (and no QC) calculations were carried out since the long-time propagation of a trajectory is needed to distinguish between dissociation and no reaction. Except at low energies ($E<8$ eV), the collisions are always reactive, i.e., either protonium formation or dissociation. This peculiar feature may have resulted from the collinear collision assumption. Cohen [10,11] found the molecular target to be much more efficient in protonium formation than the atomic target. Also in the present collinear collisions, Fig. 9 shows a very large probability of protonium formation even at high energies ($E\gg 13.6$ eV), unlike the case of the atomic target. This may be understood as follows. The molecule can be easily excited to the vibrational continuum by the incident antiproton when the kinetic energy is above the dissociation limit (=2.65 eV), as seen in Fig. 5. Then, promptly after that, the strong attractive Coulomb force combines the antiproton with the inner proton, promoting protonium formation.

The L dependence of the QC probability $P_{\bar{p}p}$ is also reproduced very well in the adiabatic approximation, as is found in Fig. 10 for $E=100$ eV. For small L, the attractive

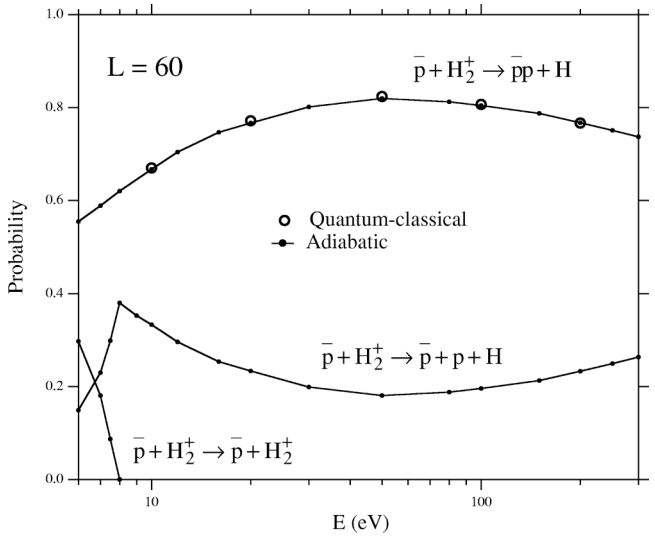

FIG. 9. Probabilities of protonium formation ($\bar{p}+H_2^+ \rightarrow \bar{p}p+H$), dissociation ($\rightarrow \bar{p}+p+H$), and nonreactive collision ($\rightarrow \bar{p}+H_2^+$) for $L=60$ calculated as functions of the collision energy E by using the quantum-classical and adiabatic-approximation methods.

interaction between the antiproton and the inner proton is so strong that a protonium atom is always formed. The critical angular momentum $L_c(\sim 67)$ for protonium formation, suggested in Sec. III, can be confirmed by the inspection of Fig. 10. As L increases beyond $\sim L_c$, protonium formation becomes negligible.

For L somewhat larger than L_c, we may expect almost all collisions to induce dissociation (2). For extremely large L, however, the collisions will be nonreactive because the attractive interaction between the antiproton and the inner proton becomes very weak. This feature is seen in Fig. 11, where the trajectories calculated in the adiabatic approximation are plotted. For $L=300$, the molecule remains bound

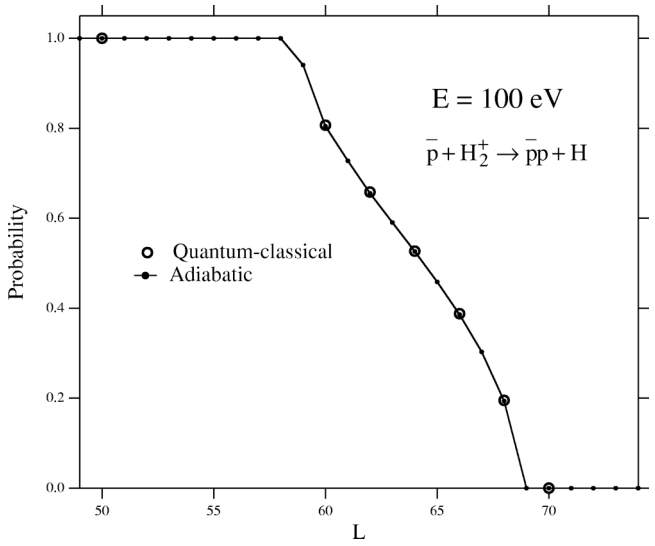

FIG. 10. Probability of protonium formation ($\bar{p}+H_2^+ \rightarrow \bar{p}p+H$) at $E=100$ eV calculated as a function of the angular momentum L by using the quantum-classical and adiabatic-approximation methods.

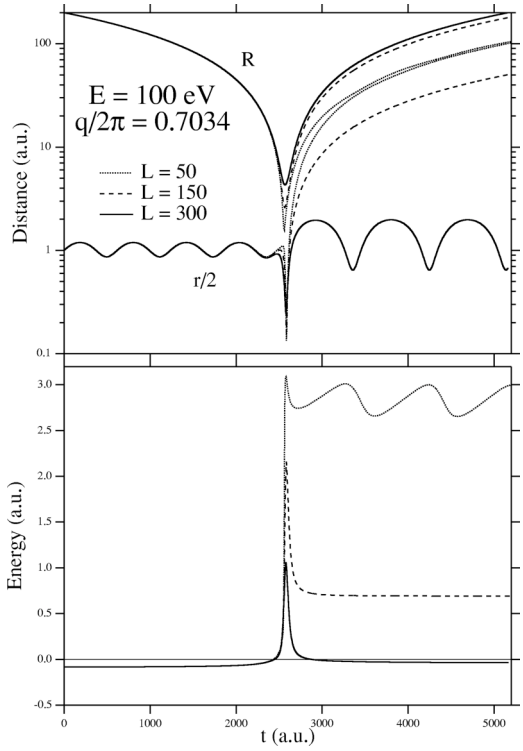

FIG. 11. Time evolution of the distances $R(t)$ and $r(t)/2$ (upper panel) and of the vibrational energy $E_{vib}(t)$ of the hydrogen molecular ion (lower panel) for $E=100$ eV, $R(t=0)=200$ a.u., $q/2\pi=0.7034$ $[r(t=0)=2.0$ a.u., $P_r(t=0)>0]$, and for three values of $L(=50,150,300)$, obtained in the adiabatic approximation.

after the collision. The lower panel of Fig. 11 shows the time dependence of the vibrational energy E_{vib} of the hydrogen molecular ion measured from the dissociation limit. The final constant vibrational energy E_{vib} is positive (meaning dissociation) for $L=150$ and negative (bound vibrational states) for $L=300$. For $L=50$, E_{vib} never approaches a constant because a protonium atom is produced.

Finally, Fig. 12 shows the probabilities of protonium formation, dissociation, and nonreactive collisions, calculated in the adiabatic approximation for $E=100$ eV as functions of

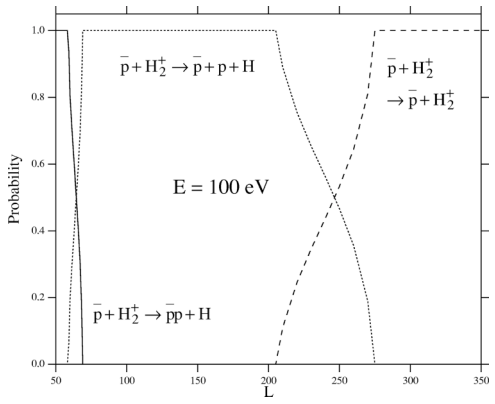

FIG. 12. Probabilities of protonium formation ($\bar{p}+H_2^+ \rightarrow \bar{p}p+H$), dissociation ($\rightarrow \bar{p}+p+H$), and nonreactive collision ($\rightarrow \bar{p}+H_2^+$) at $E=100$ eV calculated as functions of the angular momentum L in the adiabatic approximation.

$L(=50-350)$. Over a wide range of L, the probability of dissociation is almost unity. This fact confirms again the importance of vibrational excitation to the continuum in the reaction dynamics.

V. SUMMARY AND REMARKS

We have studied protonium formation in $\bar{p}+H_2^+$ collisions by assuming the collinear configuration for the three heavy particles, using both the QC (quantum-classical) hybrid method and the adiabatic approximation. We have found that the adiabatic approximation is highly satisfactory at energies much less than 1 keV. The adiabatic PES has been found to provide an almost thorough understanding of the protonium formation dynamics in low-energy collisions, just as in chemical reaction studies; vibrational excitation to the continuum at any energies higher than the dissociation energy 2.65 eV, followed by the capture of the antiproton by the inner proton, is the efficient formation mechanism. For this reason, the formation probability is appreciable even at fairly high energies. This distinguishes clearly the molecular target from the atomic target, as was indicated by the FMD study by Cohen [10,11]. It should be noted, however, that the collinear treatment might overestimate the effects of vibrational excitation. A definitive quantitative conclusion must await a 3D calculation.

An extension to 3D calculations in the adiabatic approximation would provide a deeper understanding of the dynamics including the effects of molecular rotation on protonium formation. A CTMC calculation for the 3D collisions on the adiabatic PES will be reported elsewhere [23]. However, the quantum nature of the vibrational or rotational motion must be important especially at low energies. A full quantal treatment would be also highly desirable.

For high energies ($\gtrsim$1 keV), the adiabatic approximation is no more reliable since electronic excitation and ionization are important. The QC method may still be useful in studying such high-energy collisions.

ACKNOWLEDGMENTS

The author would like to thank Professor I. Shimamura for careful reading and improving the manuscript, Professor F. Koike for discussions, and Dr. H. Takagi for providing him with a computer code for calculating the adiabatic electronic states of hydrogen molecular ions. This research was partially supported by the Grant-in-Aid for Scientific Research from the Ministry of Education, Science, Sports, and Culture of Japan.

[1] J. Eades and F. J. Hartmann, Rev. Mod. Phys. **71**, 373 (1999).
[2] M. H. Holzscheiter and M. Charlton, Rep. Prog. Phys. **62**, 1 (1999).
[3] T. Yamazaki, N. Morita, R. Hayano, E. Widmann, and J. Eades, Phys. Rep. **366**, 183 (2002).
[4] M. Amoretti *et al.*, Nature (London) **419**, 456 (2002).
[5] G. Gabrielse *et al.*, Phys. Rev. Lett. **89**, 213401 (2002).
[6] G. Gabrielse *et al.*, Phys. Rev. Lett. **89**, 233401 (2002).
[7] D. L. Morgan, Jr. and V. W. Hughes, Phys. Rev. D **2**, 1389 (1970).
[8] D. L. Morgan, Jr. and V. W. Hughes, Phys. Rev. A **7**, 1811 (1973).
[9] J. S. Cohen, Phys. Rev. A **36**, 2024 (1987).
[10] J. S. Cohen, Phys. Rev. A **56**, 3583 (1997).
[11] J. S. Cohen, Phys. Rev. A **59**, 1160 (1999).
[12] D. R. Schultz, P. S. Krstić, C. O. Reinhold, and J. C. Wells, Phys. Rev. Lett. **76**, 2882 (1996).
[13] A. Y. Voronin and J. Carbonell, Phys. Rev. A **57**, 4335 (1998).
[14] K. Sakimoto, J. Phys. B **34**, 1769 (2001).
[15] K. Sakimoto, Phys. Rev. A **65**, 012706 (2002).
[16] K. Sakimoto, Phys. Rev. A **66**, 032506 (2002).
[17] B. D. Esry and H. R. Sadeghpour, Phys. Rev. A **67**, 012704 (2003).
[18] N. H. Kwong, J. D. Garcia, and J. S. Cohen, J. Phys. B **22**, L633 (1989).
[19] K. Sakimoto, J. Phys. B **35**, 997 (2002).
[20] P. S. Krstić, D. R. Schultz, and R. K. Janev, J. Phys. B **29**, 1941 (1996).
[21] I. Shimamura, Phys. Rev. A **46**, 3776 (1992).
[22] P. T. Greenland, J. S. Briggs, and R. Thürwächter, J. Phys. B **27**, 1233 (1994).
[23] K. Sakimoto, J. Phys. B (to be published).
[24] W. Pauli, Jr., Ann. Phys. (Leipzig) **68**, 177 (1922).
[25] G. Jaffé, Z. Phys. **87**, 535 (1934).
[26] D. R. Bates, K. Ledsham, and A. L. Stewart, Philos. Trans. R. Soc. London, Ser. A **246**, 215 (1953).
[27] C. L. Pekeris, Platinum Met. Rev. **112**, 1649 (1958).
[28] D. Baye and P. H. Heenen, J. Phys. A **19**, 2041 (1986).
[29] J. C. Light, I. P. Hamilton, and J. V. Lill, J. Chem. Phys. **82**, 1400 (1985).
[30] K. Sakimoto, J. Phys. B **33**, 5165 (2000).
[31] F. Calogero, J. Math. Phys. **22**, 919 (1981).